

Climate Change and Sustainable Energy Strategies in Afyonkarahisar: A Temperature Forecasting Approach

Feyza Nur YEŞİL^{1*}, Tuba Nur SERTTAŞ²

Abstract

Climate change, which results in rising global temperatures, poses a significant threat to Turkey, particularly regarding drought. Increasing temperatures not only jeopardize human health but also facilitate the spread of infectious diseases, disrupt ecological cycles, create irregular precipitation patterns, diminish agricultural productivity, and worsen resource scarcity. Consequently, monitoring temperature trends is essential for enhancing agricultural lands, conserving water resources, implementing sustainable energy initiatives, and formulating effective climate action plans. In this context, the present study focuses on temperature forecasting for Afyonkarahisar, a region of strategic importance for agriculture and renewable energy. Hourly temperature data from 2018 to 2022, obtained from the Afyonkarahisar Meteorological Service, were utilized to implement ARIMA and SARIMA models based on Box-Jenkins methods. The Seasonal Naive Forecast model was used as a basic benchmark to demonstrate the predictive capabilities of these models. Their performance was comparatively analyzed by using performance metrics evaluated over quarterly periods for the last year. The developed ARIMA(2,1,1) model outperformed the SARIMA(2,1,1)(1,1,2)₁₂ model, achieving improvements of 11.06% in RMSE, 10.80% in MAE, and 10.92% in R²; additionally, it surpassed the Seasonal Naive Forecast model with improvements of 60.59% in RMSE and 61.89% in MAE. The experimental results demonstrate that the ARIMA model effectively captures seasonal temperature trends and variations, providing accurate and cost-effective long-term forecasts.

Keywords: Air temperature predict, Box-Jenkins, ARIMA, SARIMA, Climate changes.

Afyonkarahisar'da İklim Değişikliği ve Sürdürülebilir Enerji Stratejileri: Sıcaklık Tahmin Yaklaşımı

Öz

Küresel sıcaklıkların artmasına neden olan iklim değişikliği, özellikle kuraklık açısından Türkiye için ciddi bir tehdit oluşturmaktadır. Artan sıcaklıklar yalnızca insan sağlığını tehlikeye atmakla kalmaz; aynı zamanda bulaşıcı hastalıkların yayılmasını hızlandırır, ekolojik döngüleri bozar, düzensiz yağış modelleri oluşturur, tarımsal verimliliği azaltır ve kaynak kıtlığını daha da kötüleştirir. Bu nedenle, sıcaklık eğilimlerinin izlenmesi; tarımsal alanların iyileştirilmesi, su kaynaklarının korunması, sürdürülebilir enerji girişimlerinin uygulanması ve etkili iklim eylem planlarının oluşturulması için önemlidir. Bu bağlamda, mevcut çalışma tarım ve yenilenebilir enerji açısından stratejik öneme sahip bir bölge olan Afyonkarahisar için sıcaklık tahminine odaklanmaktadır. Afyonkarahisar Meteoroloji Müdürlüğü'nden alınan 2018-2022 yılları arasındaki saatlik sıcaklık verileri, Box-Jenkins yöntemlerine dayalı ARIMA ve SARIMA modellerini uygulamak için kullanılmıştır. Bu modellerin tahmin yeteneklerini göstermek için temel bir kıyaslama olarak Mevsimsel Naif Tahmin modeli kullanıldı. Performansları, son yıl için çeyreklik dönemler üzerinden performans ölçütleri kullanılarak karşılaştırmalı olarak analiz edildi. Geliştirilen ARIMA(2,1,1) modeli, SARIMA(2,1,1)(1,1,2)₁₂ modelini geride bırakarak RMSE'de %11,06, MAE'de %10,80 ve R²'de %10,92 iyileştirme elde etti; ayrıca, RMSE'de %60,59 ve MAE'de %61,89 iyileştirmelerle Mevsimsel Naif Tahmin modelini geçti. Deneysel sonuçlar, ARIMA modelinin mevsimsel sıcaklık eğilimlerini ve değişimlerini etkili bir şekilde yakalayarak maliyet açısından uygun, uzun vadeli doğru tahminler sağladığını göstermektedir.

Anahtar Kelimeler: Hava sıcaklık tahmini, Box-Jenkins, ARIMA, SARIMA, İklim değişikliği.

¹Afyon Kocatepe University, Technology Faculty, Electrical – Electronic Engineering, Afyonkarahisar, Turkey, fyesis@aku.edu.tr

²Afyon Kocatepe University, Technology Faculty, Electrical – Electronic Engineering, Afyonkarahisar, Turkey, tngul@aku.edu.tr

*Sorumlu Yazar/Corresponding Author

1. Introduction

Global warming and climate change are among the most debated topics of the 21st century and have been the subject of numerous scientific articles. This issue is not only a major focus within the scientific community but also among governments and international organizations. The Intergovernmental Panel on Climate Change (IPCC), in its Fifth Assessment Report, unequivocally emphasized that climate change and global warming are undeniable scientific facts (Fu, 2022). Climate change is a complex system that sustains a habitable environment for living organisms. This system comprises the atmosphere, glaciers, frozen land masses, land surfaces, oceans, other water bodies, and living organisms, all of which constantly interact with each other. Statistically significant long-term changes in the average state or variability of the climate are defined as climate change (Türkeş, 1997). The United Nations Framework Convention on Climate Change (UNFCCC) defines climate change as "a change in the climate that is attributed directly or indirectly to human activity, which alters the composition of the global atmosphere, in addition to natural climate variability observed over comparable time periods." (United Nations Framework Convention on Climate Change [UNFCCC], 1992). Climate change is caused by external forcing factors such as volcanic eruptions and solar radiation, as well as human-induced factors such as industrialization and the use of fossil fuels (Türkeş, 2000). Research on climate change in the literature emphasizes that the primary cause of this issue is human activity. Reports published by Intergovernmental Science-Policy Platform on Biodiversity and Ecosystem Services (IPBES) and IPCC on biodiversity and climate have shown that 77% of all land and 87% of all oceans have been directly affected by human activities. Additionally, it is noted that up to 37% of greenhouse gas emissions are attributed to human activities (Beggs, 2004). The Industrial Revolution is regarded as the onset of the Anthropocene era, as it gave rise to factors such as overconsumption, urbanization, and the inefficient use of natural resources (Polat & Kahraman, 2021). Urbanization is responsible for a substantial portion of carbon emissions, accounting for approximately 75% of carbon dioxide releases. Deforestation and improper land use adversely affect ecological systems, particularly human health. Consequently, the development of sustainable cities and communities is essential in the battle against climate change (Tuğaç, 2022). Climate change negatively impacts ecological systems, primarily affecting human health. According to the IPCC Sixth Assessment Report, global temperatures have increased by 0.99 °C since the pre-industrial period. This increase not only causes glaciers to melt and sea levels to rise but also poses a threat to biodiversity and essential resources such as food, air, and water. The United Nations has identified climate change as a global issue that needs to be addressed, affecting society economically, physiologically, and biologically (Fu, 2022). The 2022 Global Risks Report by the World Economic Forum (WEF) identifies the top three risks as the failure to address climate change, extreme weather

events, and biodiversity loss (World Economic Forum [WEF], 2022). In addition to its environmental and economic significance, climate change profoundly impacts public health. The reduction of safe water resources complicates food supply and decreases nutritional efficiency. Irregular patterns of heat and rainfall facilitate the spread of infectious diseases, while elevated carbon dioxide levels exacerbate allergic conditions (Franchini & Mannucci, 2015).

To combat climate change, sustainable development goals are set, aiming at environmental planning, resource utilization, and improving welfare levels. Developments in renewable energy have gained momentum to reduce the use of fossil fuels, achieve zero carbon emissions, and ensure clean and sustainable energy (Dinc Cavlak, 2024). Turkey is at significant risk of drought due to climate change, leading to hot weather fluctuations, the formation of floods, and the depletion of water resources. Located in the mid-latitude region, Turkey exhibits a semi-arid and semi-humid climate. To demonstrate the long-term impacts of climate change on Turkey, climate projections for the period 2016-2099 have been developed using three different global models. It is predicted that due to temperature increases, Turkey will be among the water-poor countries by 2050 (Turan, 2018). According to Turkey's Water Footprint Report (2014), 89% of water usage is attributed to agricultural activities. Consequently, the rise in abnormally high temperatures, irregular precipitation patterns, and subsequent water scarcity are expected to have the most significant impact on the agricultural sector (Demirbaş & Aydin, 2020). Due to its complex climate structure, Turkey is one of the countries most vulnerable to climate change resulting from global warming. The degree of impact varies across different regions due to the country's topographic features and orographic factors. The Southeastern and Central Anatolia regions, which are at risk of desertification, along with the semi-humid Aegean and Mediterranean regions that lack sufficient water resources, are particularly susceptible to the effects of rising temperatures (Öztürk, 2002).

Monitoring air temperature anomalies is crucial in the fight against climate change. Air temperature is a significant parameter to eliminate uncertainty in created climate scenarios, develop ecological plans and strategies, and reclaim agricultural and wetland areas. Accurate air temperature forecasting is key to mitigating the effects of climate change and associated global warming and to developing sustainable energy policies (Karabulut & Topçu, 2022). Additionally, the Turkey Action Plan includes measures to enhance the use of renewable energy and minimize carbon emissions to the lowest possible levels.

Temperature forecasting has been extensively studied across various disciplines in the literature. Machine learning (ML) models have been utilized for climate change detection (Alomar et al., 2022; Aghelpour et al., 2019; Naing & Htike, 2015; Sanikhani et al., 2018) while artificial intelligence-based (ANN) models have been employed for temperature forecasting in water resource management and agricultural planning (Salcedo-Sanz et al., 2016; Kisi & Shiri, 2014; Tektaş, 2010;

Singh et al., 2019). Recurrent Neural Networks (RNNs), known for their capability to process sequential data inputs, have proven effective in analyzing temperature time series (Nketiah et al., 2023; Huang et al., 2019). However, RNNs face limitations in retaining information in long-term memory due to the vanishing gradient problem (Singh et al., 2019). To address this issue, the Long Short-Term Memory (LSTM) architecture was specifically developed, and it has become one of the most preferred deep neural network models due to its high accuracy in forecasting (Ozbek et al., 2021; Park et al., 2019; De Saa & Ranathunga, 2020; Sekertekin et al., 2021; Zaytar & El Amrani, 2016; Li & Yang, 2023). In a temperature forecasting study conducted for the Chinese region, deep learning-based approaches were shown to better capture irregular and nonlinear relationships within the time series (Shen et al., 2020). Similarly, Lai et al. emphasized that the Autoregressive Integrated Moving Average (ARIMA) model, a statistical approach they proposed for developing regional climate models, is a reliable and interpretable forecasting method (Lai & Dzombak, 2020). Another study employing the ARIMA model focused on long-term temperature forecasting to detect climate change in developing countries (Amjad et al., 2022; Islam & Zakaria, 2019). Time series regression models proposed for four regions with different climatic characteristics demonstrated consistent forecasting performance by accounting for seasonal and trend features of the data (Murat et al., 2018). Moreover, the Variational Mode Decomposition (VMD) technique, which extracts trends, noise, and dependent relationships within the time series, significantly enhanced the forecasting capability of the ARIMA model (Wang et al., 2019). The use of heuristic optimization algorithms and hybrid models that combine multiple methods has also been shown to reduce forecasting errors, making them among the preferred techniques in temperature forecasting studies (Thi Kieu Tran et al., 2020; Haque et al., 2021; Hou et al., 2022; Roy, 2020). Hybrid models that integrate various forecasting methods or AI-based approaches utilizing deep neural networks are recommended for enhanced accuracy. However, these models can be complex and computationally demanding. Furthermore, AI-based models often face challenges related to interpretability, which can adversely impact model transparency. By contrast, the Box-Jenkins models, as a statistical approach, are inherently interpretable. The dynamics of the models can be analyzed through its AR, MA, and seasonal terms. Deep learning models often require substantial computational resources during the training phase, while the Box-Jenkins methods offer a simpler and more flexible structure in terms of parameter tuning and forecasting processes. Deep learning methods generally need large datasets to improve generalization and uncover meaningful relationships, whereas the Box-Jenkins models can perform well even with limited data. Furthermore, the Box-Jenkins models are particularly preferred in cases with seasonal cycles, such as climate datasets, due to its effective seasonal component capture. Based on these reasons, the Box-Jenkins models have been recommended for time series forecasting of air temperature in this study.

In this context, daily temperature forecasts were made for Afyonkarahisar province to monitor seasonal temperature changes. Forecasting models were developed using the Box-Jenkins methods, specifically ARIMA and Seasonal Autoregressive Integrated Moving Average (SARIMA), which are widely used for time series forecasting. In addition, the Seasonal Naive Forecast model was employed as a comparative model to demonstrate the forecasting accuracy of these models. This study utilized hourly air temperature data collected from 2018 to 2022, obtained from the Afyonkarahisar Meteorological Service. The performance of the developed models was evaluated comparatively using various performance assessment metrics to analyze their forecasting capabilities. Afyonkarahisar, situated in the TR33 region and classified as a moderate-risk area, holds significant geopolitical importance for agriculture, livestock, and industry. Drought analysis is especially important for agricultural activities, including the cultivation of cherries, potatoes, poppies, and sour cherries. This study aims to emphasize the significance of air temperature forecasting for sustainable energy and climate action plans in Afyonkarahisar. By taking into account temperature fluctuations, monitoring water resources and agricultural land becomes possible, and solar energy projects can be initiated. This facilitates adjustments in environmental policies and the generation of job opportunities in the renewable energy sector. It also enables researchers to draw inferences for regions with similar climate characteristics, offering insights for those working in this field. In the current study, using a univariate time series significantly reduces model complexity and cost. Due to its flexibility, the model is open to optimization for future research.

The organization of the paper is planned as follows: Section 2, under the methods heading, details the data used, time series stationarity tests, and the structure of the Box-Jenkins models and Seasonal Naïve Forecast model. Section 3 presents the data preparation process, performance evaluation criteria, and experimental studies. Finally, last section includes the results and discussion section, which analyzes the experimental studies and findings.

2. Materials and Methods

Afyonkarahisar is located at the coordinates 30°28'–30°38' East and 38°42'–38°50' North, with an elevation of 1,021 meters. Located in the Inner Western Anatolia Region of the Aegean Region, this area experiences a harsh continental climate due to its altitude. Its distance from the sea and low humidity levels contribute to moderate precipitation. According to data from the Afyon Meteorology Service, the city's annual average temperature is 11.2°C, and it receives an average annual precipitation of 444 mm. In this study, monthly air temperature forecast was made using hourly air temperature data in Afyonkarahisar between 2018-2022. Box-Jenkins method was preferred for the

time series forecast model. This section provides information about the dataset used, the applied methodologies and the performance evaluation metrics used.

2.1. Data Used

This study presents a time series forecast model to perform monthly air temperature forecast for Afyonkarahisar. The purpose of the forecast model is to detect climate change and contribute to sustainable energy research. Hourly temperature data between 2018-2022 obtained from Afyonkarahisar Meteorological Service were converted to daily averages by calculating 24-hour average temperatures. The time series graph shown in Figure 1 shows the daily temperature values for Afyonkarahisar province. At certain time points, the temperature values exhibit sudden trends of either increase or decrease. This indicates that the series has non-stationary variance and mean. As the values increase from the first month of the year to the 6th month and decrease towards the 12th month, it can be inferred that the time series exhibits seasonal movement with similar trends across specific periods.

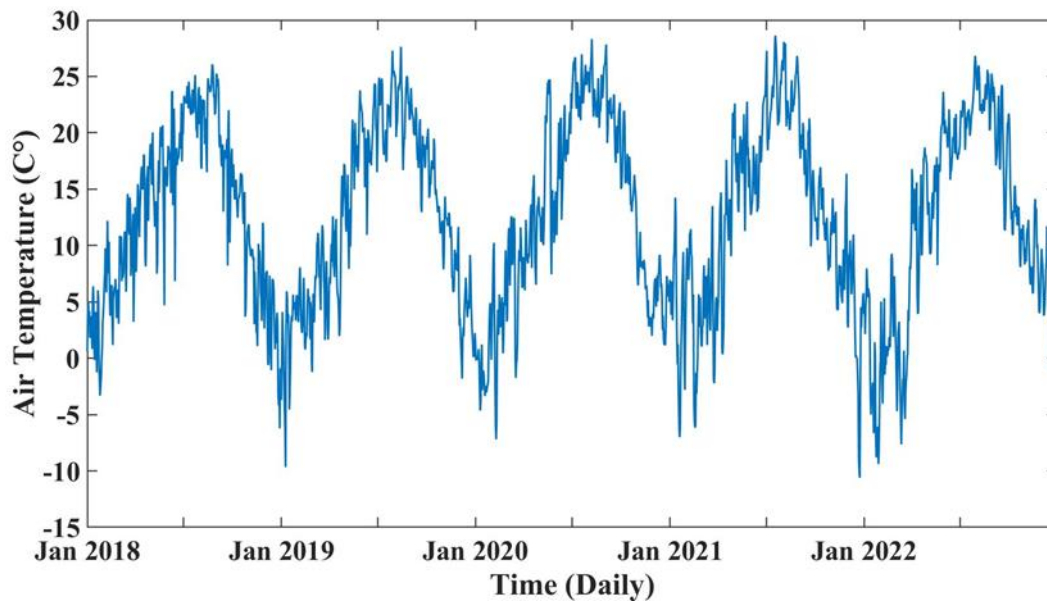


Figure 1. Daily average air temperature values measured in Afyonkarahisar between 1 jan, 2018 – 31 Dec, 2022.

The statistical measures of the temperature time series, which consists of 1,826 observations, are presented in Table 1.

Table 1. Descriptive statistical measures for air temperature time series.

Maximum	Minimum	Median	Mean	Standard Deviation	Variance	Skewness	Kurtosis
28.625	-10.604	12.54	12.448	8.292	68.758	-0.196	2.129

The difference between the maximum and minimum values indicates high variability in the time series. The proximity of the mean value to the median suggests a symmetric data distribution. The average temperature was recorded at 12.54°C, indicating an upward trend in temperature values compared to previous years. A high standard deviation and variance demonstrate that the temperature time series is non-stationary. Skewness and Kurtosis are statistical measures used to assess the distributional characteristics of time series data (Joanes & Gill, 1998). Skewness analyzes the symmetry of the data distribution. A positive skewness value indicates that the data distribution is skewed to the right, while a negative skewness value indicates that it is skewed to the left. If the skewness value is zero, it signifies a symmetric distribution. For the temperature time series, a slightly negative skewness value was obtained, indicating that extreme values are limited and the distribution is generally close to normal. Kurtosis is used to evaluate the presence of extreme values in the data distribution. If the kurtosis value is greater than three, the dataset contains more outliers; conversely, if it is less than three, the dataset exhibits a distribution where outliers have less impact. A kurtosis value exactly equal to three indicates a normal distribution. For the temperature time series, a kurtosis value of less than three was obtained, indicating that the dataset does not contain a significant number of outliers and reflects a relatively normal distribution.

To apply the Box-Jenkins methods, the time series must be stationary. Therefore, it is essential to conduct a stationarity test on the time series before designing the model. Time series with a constant mean and variance are considered stationary stochastic processes. In the literature, the Dickey-Fuller unit root test (Dickey & Fuller, 1979) and the Kwiatkowski-Phillips-Schmidt-Shin (KPSS) test (Kwiatkowski et al., 1992) are commonly used to analyze the stochastic properties of time series. For the stationarity test of the temperature time series, both the ADF test and the Kwiatkowski- KPSS test were conducted, with the results presented in Table 2. The ADF test operates under the null hypothesis (H_0) that the series contains a unit root, while H_0 of the KPSS test posits that the series is stationary. If the p-value falls below the critical threshold of 0.05, the H_0 is rejected. Statistically significant results were obtained for both tests, leading to the rejection of the H_0 . This outcome indicates that the time series is non-stationary. The presence of seasonal patterns in the temperature time series contributes to its lack of stationarity.

Table 2. ADF and KPSS test results of air temperature time series.

Test	Null Hypothesis (H_0)	Null Rejected	P-Value
ADF	Air temperature time series contains a unit root.	True	1.000e-03
KPSS	Air temperature time series is trend stationary.	True	0.0100

To achieve stationarity in a time series, techniques such as differencing and logarithmic transformations can be employed. In this study, differencing was applied to eliminate the seasonal

component from the temperature time series. Table 3 presents the results of the KPSS and ADF tests conducted following the differencing process. The KPSS test yielded a p-value above the critical threshold of 0.05, indicating a significant result. Consequently, the H_0 cannot be rejected in favor of the alternative hypothesis. This outcome suggests that the temperature time series has achieved stationarity.

Table 3. ADF and KPSS test results of air temperature time series after differencing process.

Test	Null Hypothesis (H_0)	Null Rejected	P-Value
ADF	Air temperature time series contains a unit root.	True	1.000e-03
KPSS	Air temperature time series is trend stationary.	False	0.100

Figure 2 illustrates the time series graph of the air temperature data obtained after applying differencing and seasonal differencing. When Figure 2 is examined, it is observed that the temperature time series generally fluctuates around zero. Although it exhibits higher amplitude fluctuations in certain periods, no significant variance changes occur. The seasonal effect has noticeably disappeared, and no increasing or decreasing trend is observed. In addition to the visual assessment, the results of the ADF and KPSS tests confirm that the temperature time series has become stationary after differencing processes.

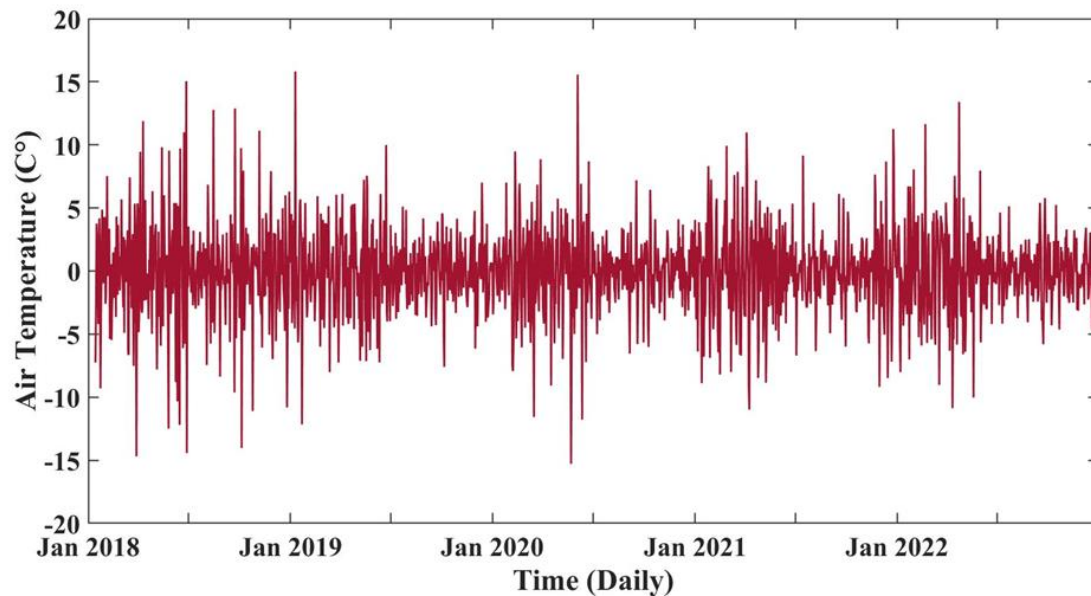


Figure 2. Daily average air temperature time series plot after differencing process.

2.2. Box-Jenkins Method

Time series are formed by the chronological ordering of data observed at equal intervals. Time series forecasting involves examining past data to make predictions about the future. A time series is considered stationary if it has a constant mean and variance. For univariate stochastic processes, Box-Jenkins methods are used.

2.2.1. Autoregressive Integrated Moving Average (ARIMA) model

Time series may lose their stationarity due to their characteristics such as trend and seasonal movement or external reasons such as natural disaster, pandemic, economic crisis (Hamilton, 2020). The ARIMA model, one of the Box-Jenkins methods, is used for the analysis of non-stationary time series. The ARIMA model is shown with the notation ARIMA(p,d,q). The autoregressive component is expressed as AR(p), which defines the relationship between the current value and the lagged values. The moving average component is represented as MA(q) and accounts for the lagged values of the estimation errors. The term I(d) signifies the integrated component, indicating the order of differencing applied to achieve stationarity in the time series. The ARIMA(p,d,q) model is expressed as follows:

$$y_t = \phi_1 y_{t-1} + \phi_2 y_{t-2} + \dots + \phi_p y_{t-p} + \varepsilon_t - \theta_1 e_{t-1} - \dots - \theta_q e_{t-q} \quad (1)$$

Here, y_t is stationary time series at the t time; $y_{t-1}, y_{t-2}, \dots, y_{t-p}$ represent the past values of the series; $\phi_1, \phi_2, \dots, \phi_p$ are the AR coefficients; $\theta_1, \dots, \theta_q$ are the MA coefficients; ε_t is error term at the t time; e_{t-1}, \dots, e_{t-q} represent the past error term.

$$\nabla^d x_t = y_t = (1 - B)^d x_t \quad (2)$$

Here, x_t is the original time series, y_t is stationary time series, $\nabla^d x_t$ or $(1 - B)^d x_t$ is the d-th order differenced time series. B is the backshift operator. B shifts the series by one time step, such that $Bx_t = x_{t-1}$.

2.2.2. Seasonal Autoregressive Integrated Moving Average (SARIMA) model

Seasonal Autoregressive Integrated Moving Average (SARIMA), a method developed by Box and Jenkins, is designed to analyze time series data that exhibit seasonal patterns. In addition to the

standard ARIMA parameters, SARIMA incorporates seasonal parameters represented by the symbols (P, D, Q, s) (Box & Jenkins, 1970). The notation SARIMA(p, d, q)(P, D, Q, s) is defined as follows:

$$\phi_p(B)\Phi_P(B^s)(1-B)^d(1-B^s)^D X_t = \theta_q(B)\Theta_Q(B^s)\varepsilon_t + c \quad (3)$$

Here, $\phi_p(B)$ is the AR polynomial, $\Phi_P(B^s)$ is the Seasonal Autoregressive (SAR) polynomial, $\theta_q(B)$ is the MA polynomial, $\Theta_Q(B^s)$ is the Seasonal Moving Average (SMA) polynomial, ε_t represents the white noise term, s denotes the seasonal period, and c signifies a constant term. The terms $(1-B)^d$ and $(1-B^s)^D$ represent the differencing operations applied to ensure the stationarity and seasonal stationarity of the series, respectively.

The Box-Jenkins model design process employs a systematic approach that encompasses time series stationarity testing, parameter selection, diagnostic checks, and forecasting stages. Autocorrelation and partial autocorrelation function graphs are analyzed to obtain model parameters. Potential parameter values are assessed through diagnostic checks. Once the model's suitability is established, future predictions are produced based on historical data (Alencar et al., 2018).

2.3. Seasonal Naive Forecast Method

The Seasonal Naive method is a simple baseline forecasting approach used in time series analysis. It assumes that in time series with seasonal cycles, past seasonal patterns will repeat in the future in the same manner. In other words, the value for the upcoming period is assumed to be equal to the value from the same period in the previous season (Wang & Ma, 2023). The Seasonal Naive model is formulated as follows:

$$\hat{y}_{t+s} = y_t \quad (4)$$

Here, y_t represents the time series at time t , s denotes the seasonal period and \hat{y}_{t+s} represents the next seasonal point.

In this study, the Seasonal Naive Forecast method was used as a fundamental benchmark to analyze and interpret the performance of Box-Jenkins models.

2.4. Performance Evaluation Metrics

Various performance evaluation metrics have been utilized to assess the accuracy of the forecasting models employed in this study. These evaluation metrics test how closely the forecasted results align with the actual values, thereby enabling the determination of the model's performance and reliability. The performance of the models developed using the Mean Absolute Error (MAE), Root Mean Square Error (RMSE) and Coefficient of Determination (R^2) metrics, which are widely used in time series forecasting studies, has been evaluated from different perspectives and their forecast accuracies has been compared.

2.4.1. Mean Absolute Error (MAE)

The MAE is defined as the average of the absolute differences between the predicted values and the actual values. It is suitable for measuring the overall accuracy of forecasting models. A lower MAE value indicates strong forecasting performance. The MAE is formulated as follows:

$$MAE = \frac{1}{N} \sum_{i=1}^N |Y_{predict,i} - Y_{real,i}| \quad (5)$$

Here, $Y_{predict,i}$ is the predicted value at the i -th time step, $Y_{real,i}$ is the actual value measured at the i -th time step and N is the total number of data points.

2.4.2. Root Mean Square Error (RMSE)

The RMSE is obtained by taking the square root of the mean of the squared differences between the predicted and actual values. The RMSE metric is effective in detecting large deviations in the forecasting model. As the error value approaches zero, the forecasting performance of the model improves. The RMSE value is expressed as follows:

$$RMSE = \sqrt{\frac{\sum_{i=1}^N (Y_{predict,i} - Y_{real,i})^2}{N}} \quad (6)$$

Here, $Y_{predict,i}$ is the predicted value at the i -th time step, $Y_{real,i}$ is the actual value measured at the i -th time step and N is the total number of data points.

2.4.3. Coefficient of Determination (R^2)

The R^2 represents the linear relationship between the predicted and actual values. It is used to measure the explanatory power of the forecasting model. The R^2 value ranges between zero and one, with a value closer to one indicating a high-accuracy forecasting model. The R^2 metric is formulated as follows:

$$R^2 = 1 - \frac{\sum_{i=1}^N (Y_{real,i} - Y_{predict,i})^2}{\sum_{i=1}^N (Y_{real,i} - \mu)^2} \quad (7)$$

Here, $Y_{predict,i}$ is the predicted value at the i -th time step, $Y_{real,i}$ is the actual value measured at the i -th time step, N is the total number of data points and μ is the mean of all actual values.

3. Findings and Discussion

The Box-Jenkins modeling process includes basic steps such as time series stationarity, graphical examination of the Autocorrelation Function (ACF) and Partial Autocorrelation Function (PACF), determination of model parameters, and final estimation. Under this heading, the design process for SARIMA and ARIMA models, along with an analysis of the results from estimation performance evaluation metrics.

First, hourly air temperature data for Afyonkarahisar Province from 2018 to 2022 were converted into daily air temperature values by calculating 24-hour averages. The data from 2018 to 2021 were designated as the training dataset for the estimation model. To assess the estimation performance of the model, the data from 2022 were used as the test dataset. The stationarity test for the temperature time series is conducted during the data preparation stage. The ACF and PACF plots for the original time series, which are utilized for parameter determination, are presented in below. While the ACF illustrates the correlation coefficients between the series and its lags, the PACF displays the autocorrelation between two lagged observations exclusively. When examining the ACF plot presented in Figure 3, it is evident that the autocorrelation values decrease gradually. This observation suggests that the time series exhibits a trend or is non-stationary. Consequently, first-order differencing of the series is necessary. Given the absence of a sudden drop, the MA{0} or MA{1} coefficient can be selected. Conversely, upon analyzing the PACF plot shown in Figure 4, it is noted that autocorrelation decreases sharply after the initial few lags. This indicates that the AR{1} or AR{2} coefficient can be selected.

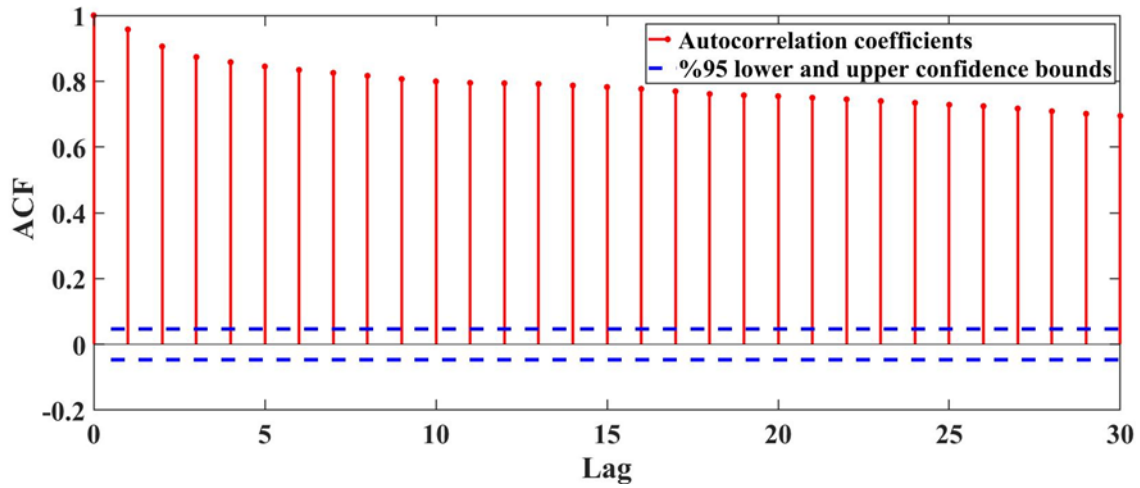


Figure 3. The ACF graph original air temperature time series.

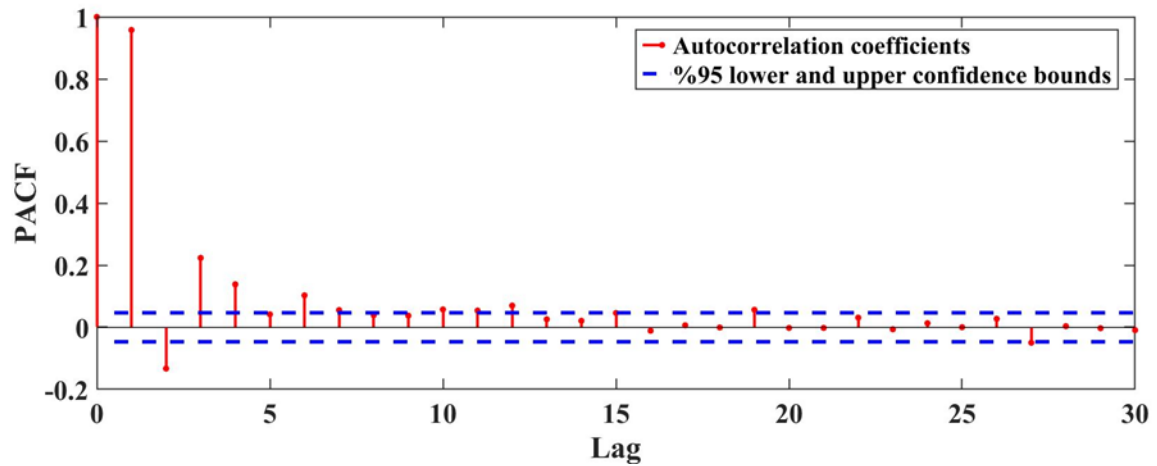


Figure 4. The PACF graph original air temperature time series.

For the selection of seasonal parameters, the seasonal ACF and seasonal PACF plots were analyzed after applying seasonal differencing to the original time series. Figure 5, illustrates the PACF graph. The graph indicates that autocorrelation decreases rapidly after the initial few lags. In this scenario, either the $SMA\{1\}$ or $SMA\{2\}$ coefficient can be selected. Similarly, the seasonal PACF graph in Figure 6 shows increases at both the 1st and 12th lags. This indicates the necessity of a seasonal AR term. The $SAR\{P\}$ coefficient can be selected as 1.

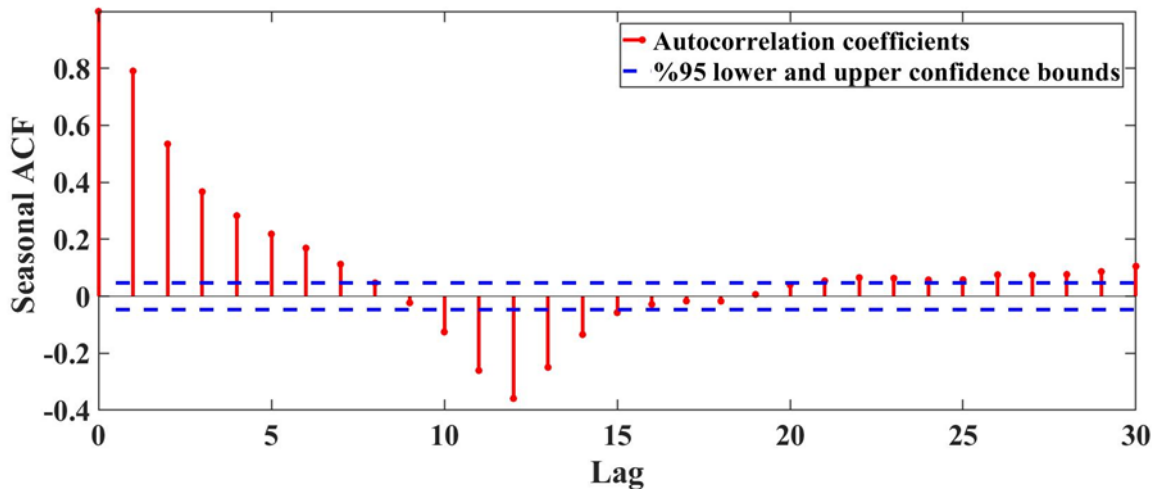


Figure 5. The ACF graph of the seasonally differenced air temperature time series.

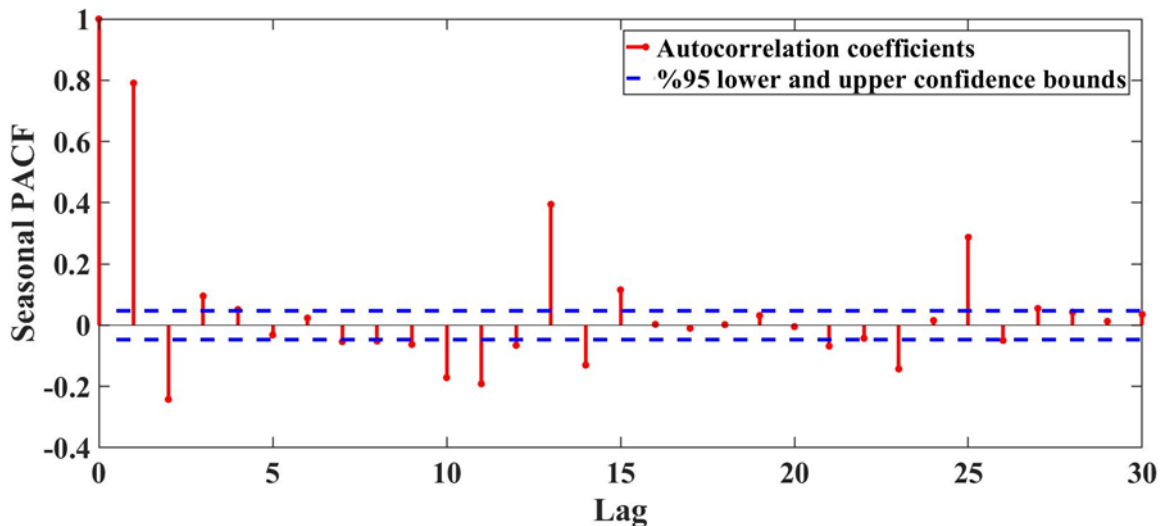


Figure 6. The PACF graph of the seasonally differenced air temperature time series.

The Akaike Information Criterion (AIC) and the Bayesian Information Criterion (BIC) are used to assess model parameters. These two criteria provide information about the fit and complexity of the model. Developed by the Japanese statistician Hirotugu Akaike in 1973, AIC aims to balance model complexity with the fit to the data. A lower AIC value indicates a more effective model design (Akaike, 1974). In the equations presented below, k represents the number of parameters in the model, L denotes the maximum likelihood function of the model, and n signifies the number of observations in the dataset.

The AIC is represented as follows:

$$AIC = 2k - 2 \ln(L) \tag{8}$$

The Bayesian Information Criterion (BIC), developed by Gideon E. Schwarz in 1978, evaluates both model fit and complexity. However, it tends to be more conservative, particularly favoring simpler models (Schwarz, 1978).

The BIC is expressed as follows:

$$BIC = \ln(n) k - 2 \ln(L) \tag{9}$$

The AIC and BIC values are evaluation criteria that do not have absolute threshold values but are solely used for model comparison. These criteria do not have a fixed lower or upper limit, as they vary depending on the dataset used and the complexity of the model. Therefore, various ARIMA and SARIMA model scenarios were developed to identify the most suitable parameter values. The AIC and BIC values of the constructed models are presented in Table 4.

Table 4. The AIC and BIC values of trained with different parameters ARIMA and SARIMA models.

Model	AIC	BIC
ARIMA(1,1,0)	8.3618e+03	8.3729e+03
ARIMA(1,1,1)	8.3328e+03	8.3494e+03
ARIMA(1,1,2)	8.1579e+03	8.1800e+03
ARIMA(2,1,0)	8.2514e+03	8.2679e+03
ARIMA(2,1,1)	8.1558e+03	8.1778e+03
ARIMA(2,1,2)	8.1527e+03	8.1802e+03
SARIMA(2,1,1)x(1,1,0) ₁₂	8.8370e+03	8.8645e+03
SARIMA(2,1,1)x(1,1,1) ₁₂	8.3151e+03	8.3481e+03
SARIMA(2,1,1)x(1,1,2)₁₂	8.2355e+03	8.2740e+03
SARIMA(2,1,1)x(2,1,0) ₁₂	8.6161e+03	8.6490e+03
SARIMA(2,1,1)x(2,1,1) ₁₂	8.3146e+03	8.3531e+03
SARIMA(2,1,1)x(2,1,2) ₁₂	8.2360e+03	8.2799e+03

The ARIMA(2,1,1) and the SARIMA(2,1,1)x(1,1,2)₁₂ model, which had the lowest AIC and BIC values, was selected. Table 5 presents the statistical values of the selected ARIMA model parameters. The statistical significance of the AR{1}, AR{2}, and MA{1} coefficients has been confirmed based on their t-statistics (34.0586, -14.9305, and -38.1956, respectively). Since the absolute magnitudes of these values are considerably greater than zero and their corresponding p-values are below the 5% significance level, these coefficients are considered statistically significant. This finding indicates that past values and past error terms have a significant impact on the temperature time series. As the first-order difference of the series was applied, the constant term is zero.

Table 5. The parameter values of ARIMA(2,1,1)

Parameter	Value	Standard Error	t Statistic	P-Value
Constant	0	0	-	-
AR{1}	0.8771	0.0258	34.0586	0.0000
AR{2}	-0.2839	0.0190	-14.9305	0.0000
MA{1}	-0.8354	0.0219	-38.1956	0.0000
Variance	5.0745	0.1123	45.1681	0

Table 6 presents the statistical values of the selected SARIMA model parameters. The t-statistics for SAR{12} (-12.7811), SMA{12} (-3.1889), and SMA{24} (-13.1392) are significantly large in magnitude, and their corresponding p-values are below the 0.05 significance level. Therefore, these coefficients are considered statistically significant. This indicates that the selected SARIMA model effectively captures the seasonal variations in the temperature time series. All coefficients are statistically significant. The inclusion of seasonal components has increased the model's variance. In this case, the most suitable model is determined based on forecasting performance results and diagnostic control graphs.

Table 6. The parameter values of SARIMA(2,1,1)x(1,1,2)₁₂

Parameter	Value	Standard Error	t Statistic	P-Value
Constant	0	0	-	-
AR{1}	0.8590	0.0263	32.6162	0.0000
AR{2}	-0.2869	0.0185	-15.5172	0.0000
SAR{12}	-0.7548	0.0591	-12.7811	0.0000
MA{1}	-0.8248	0.0206	-39.9809	0
SMA{12}	-0.1882	0.0590	-3.1889	0.0014
SMA{24}	-0.7415	0.0564	-13.1392	0.0000
Variance	5.2835	0.1187	44.5203	0

In the modeling process, various graphs are utilized for performance evaluation and error analysis. These include the R-squared plot, histogram distribution, correlogram and quantile-quantile (Q-Q) plot of residuals. The R-squared plot illustrates the relationship between the model's predicted values and the actual data. The histogram distribution assesses the distribution of the model's error terms; ideally, these error terms should conform to a normal distribution. The autocorrelation plot investigates the time-dependence of the error terms. Time-dependent residuals indicate the presence of nonlinear relationships within the model, which is an undesirable situation that can diminish the model's accuracy.

Figure 7 presents the R² plot and histogram distribution graphs for the comparative analysis of the developed models. Figure 7a. demonstrates that the ARIMA model exhibits a stronger linear relationship between the predicted and observed values. Similarly, Figure 7b. shows that the histogram curve of the ARIMA model aligns more closely with the normal distribution. However,

the histogram curve does not perfectly coincide with the red line. This discrepancy arises from the inherent deviations and errors present in the real-world temperature time series data.

Figure 8 illustrates the autocorrelation and quantile-quantile plots of the models. In Figure 8a. it is evident that the ARIMA error terms remain within the confidence intervals and demonstrate lower autocorrelation. Upon analyzing Figure 8b. it is observed that the ARIMA error terms are more closely aligned with a normal distribution. In contrast, the deviations at the extreme points in the SARIMA and Seasonal Naive Forecast models are more pronounced. Collectively, these indicators suggest that the ARIMA model exhibits superior generalization and forecasting capabilities with respect to the data.

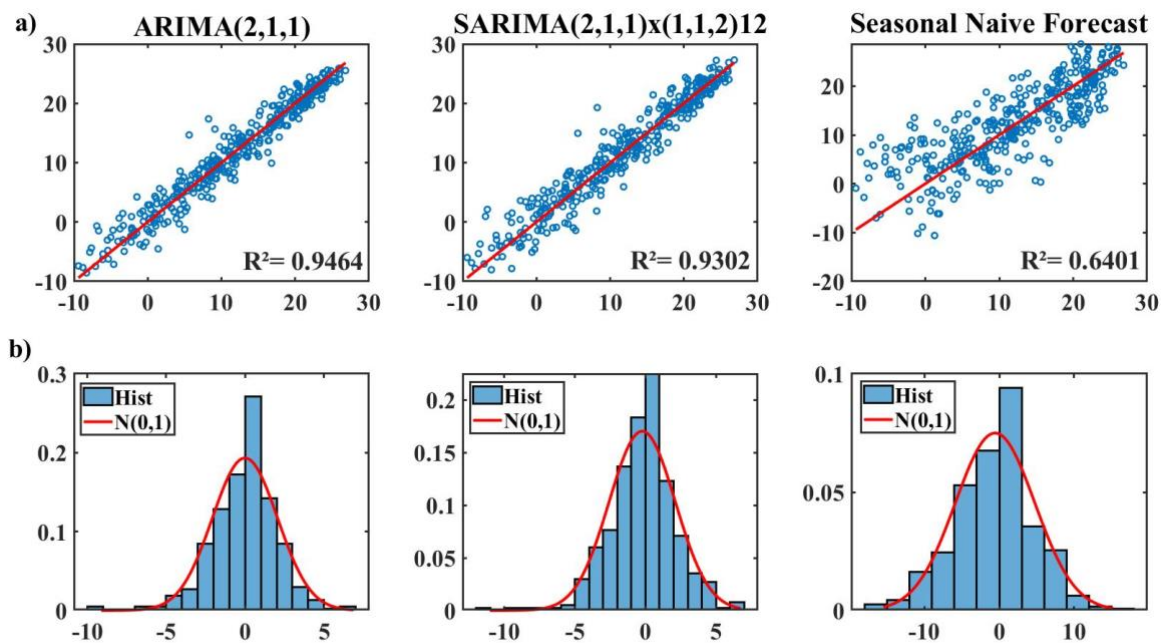


Figure 7. a) Correlation plot of residuals of ARIMA, SARIMA and Seasonal Naive Forecast models.
b) Histogram plot of residuals of ARIMA, SARIMA and Seasonal Naive Forecast models.

The daily temperature time series for 2022 was divided into four quarters to assess seasonal forecasting performance. The first quarter comprises January, February, and March; the second quarter includes April, May, and June; the third quarter consists of July, August, and September; and the fourth quarter encompasses October, November, and December. The forecasting graphs for these quarters are presented in Figures 9. Table 7 provides the results of the forecast performance metrics for the four quarters. The analysis of the data reveals an upward trend in temperature values during the first and second quarters, while a downward trend is observed in the third and fourth quarters. The ARIMA model has consistently captured the seasonal transitions. In the third quarter, the ARIMA model achieved the lowest error values, with the RMSE of 1.4231 and the MAE of 1.1326.

The highest R^2 value, 0.8492, was recorded by the ARIMA model in the fourth quarter. Achieving R^2 scores above 0.65 across all quarters indicates that the proposed ARIMA model fits the data well and effectively captures temperature trends. When averaging across quarterly periods, the ARIMA model outperformed the SARIMA model, achieving improvements of 11.06% in RMSE, 10.80% in MAE, and 10.92% in R^2 ; outperformed the Seasonal Naive Forecast model achieving improvements of 60.59% in RMSE, 61,89% in MAE.

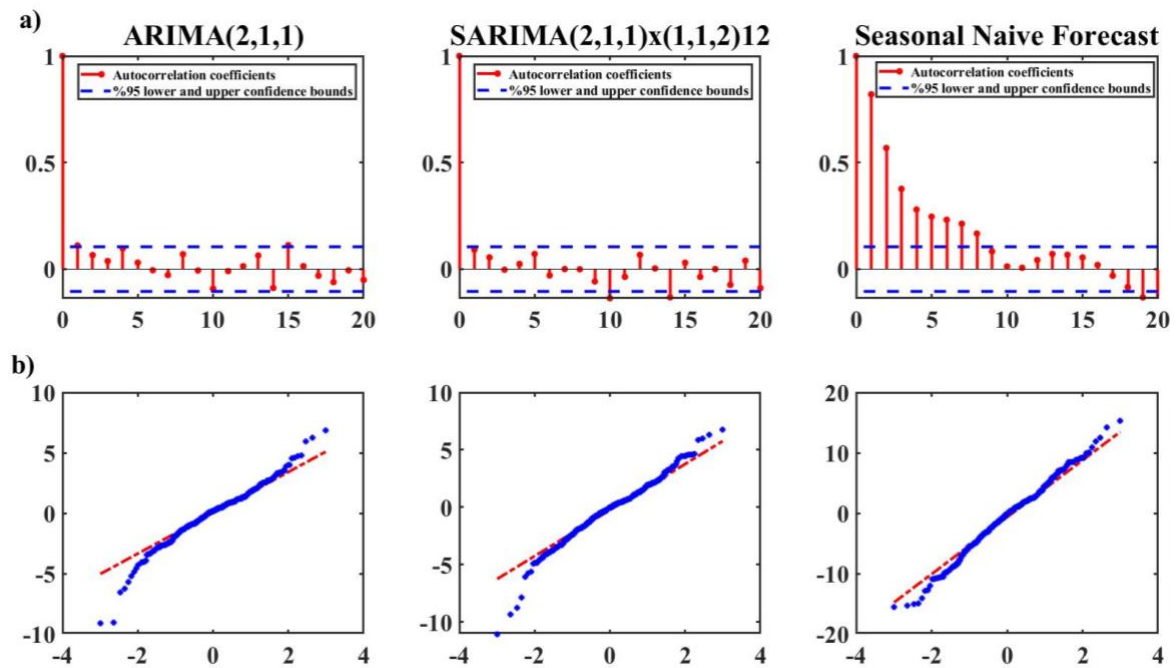


Figure 8. a) Correlogram plot of the residuals of ARIMA, SARIMA and Seasonal Naive Forecast models. b) Quantile-quantile plot of the residuals of ARIMA, SARIMA and Seasonal Naive Forecast models.

The TR33 region, where the province of Afyonkarahisar is situated, is of significant importance to Turkey due to its agricultural and renewable energy potential. The temperature forecasting study conducted using the ARIMA model aims to meet the region's needs by assisting renewable and sustainable energy planning, water and resource management, agricultural production planning, and adaptation strategies to climate change. Analysis of forecast graphs indicates that the results obtained from the proposed ARIMA model closely match actual temperature values, significantly contributing to the advanced planning of energy production and consumption in the energy sector. The forecast analysis demonstrates an upward trend in temperature values starting from March, followed by a decline after September. Particularly in August, temperatures on certain days are expected to exceed 24°C . This insight serves as an important tool for planning energy supply to meet the rising cooling demands during summer months in Afyonkarahisar and devising appropriate irrigation strategies necessary for agricultural activities. Forecast accuracy, especially during spring and summer, helps

farmers efficiently schedule planting, irrigation, and harvesting periods. High temperatures may increase water usage. The proposed forecasting model provides early warnings regarding agricultural water use, ensuring the sustainable management of water resources. In addition, high summer temperatures create favorable conditions for solar energy projects. Solar energy systems established in the region are an important resource for sustainable clean energy.

The forecasts also indicate temperatures dropping below 0°C during January and February, with a continuing downward trend from October until the end of the year. This trend highlights increased energy demand for heating and potential challenges for agricultural activities due to low temperatures. Forecast accuracy during autumn and winter contributes to energy management by predicting energy demand and supports the adoption of measures such as greenhouse farming practices to counteract the impact of declining temperatures on crop production cycles.

An examination of temperature time series data from 2018 to 2022 reveals an increasing trend in temperature values over the last five years. These fluctuations in temperature may be considered tangible evidence of climate change. Thus, climate adaptation planning can be developed specifically for Afyonkarahisar. Promoting the installation of solar panels as part of renewable energy initiatives can facilitate the transition to sustainable electricity production. Rising temperatures may adversely affect yields of traditional agricultural products; therefore, adopting alternative agricultural products resistant to climate change and drought conditions is advisable. Increasing urban green spaces can locally mitigate rising temperatures. Furthermore, enhancing waste management practices and supporting zero-waste projects can help reduce carbon emissions. Consequently, the implementation of climate-friendly policies will significantly contribute to achieving sustainable development goals in Afyonkarahisar. The proposed Box-Jenkins models can also be applied to regions with similar climatic characteristics, or the findings can be interpreted in a similar manner for these areas to generate insights.

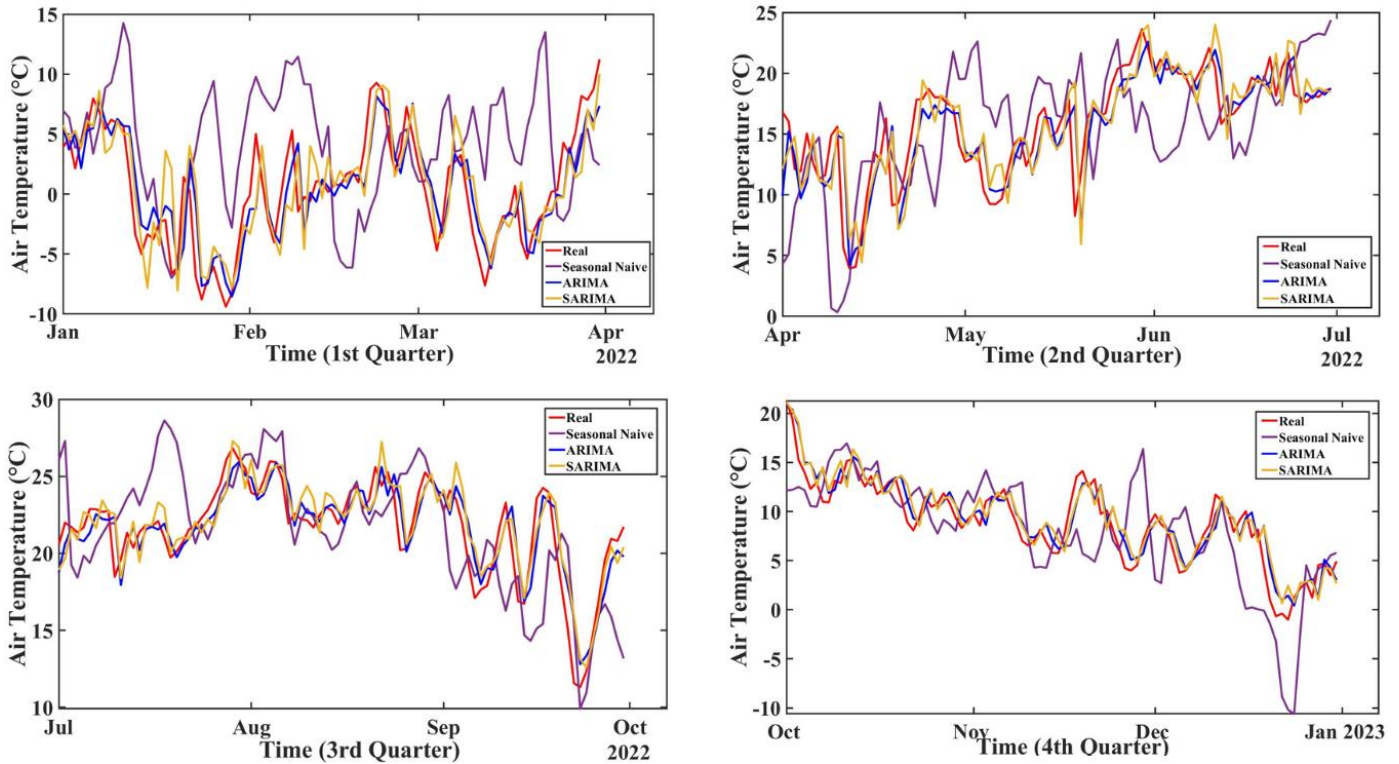


Figure 9. The forecasted results of air temperature with quarters periods.

Table 7. The results of the forecast performance metrics for the four quarters.

Quarter term	Month	Model	RMSE (°C)	MAE (°C)	R ²
1st	Jan, Feb, Mar	ARIMA(2,1,1)	2.5403	2.0017	0.7159
		SARIMA(2,1,1)x(1,1,2) ₁₂	3.0026	2.3473	0.6031
		Seasonal Naive	7.3736	6.1647	-
2nd	Apr, May, Jun	ARIMA(2,1,1)	2.4388	1.7134	0.6725
		SARIMA(2,1,1)x(1,1,2) ₁₂	2.7601	1.9748	0.5805
		Seasonal Naive	5.4058	4.4217	-
3rd	Jul, Aug, Sep	ARIMA(2,1,1)	1.4231	1.1326	0.7850
		SARIMA(2,1,1)x(1,1,2) ₁₂	1.5455	1.2208	0.7464
		Seasonal Naive	3.4818	2.7141	-
4th	Oct, Nov, Dec	ARIMA(2,1,1)	1.6244	1.3162	0.8492
		SARIMA(2,1,1)x(1,1,2) ₁₂	1.7905	1.4307	0.8168
		Seasonal Naive	4.3663	3.3331	-

Table 8 presents a comparison of the proposed Box-Jenkins approach with other machine learning-based temperature forecasting studies in the literature in terms of RMSE and MAE metrics. This analysis demonstrates that the current study achieves meaningful and sufficient accuracy.

Table 8. Comparison of some ML forecasting models found in the literature and the current model for estimating air temperature.

Ref	Input	Forecasting Model	Forecast Horizon	Location	RMSE (°C)	MAE (°C)
(Alomar et al., 2022)	Daily air temperature value between 2000-2015	Random Forest	Monthly	North Dakota, North America	2.726	-
(Aghelpour et al., 2019)	Monthly air temperature value between 1951-2011	Support Vector Machine	Monthly	Tabriz, Iran	1.881	-
(Naing & Htike, 2015)	Monthly Minimum Temperature value between 2000-2012	Multiple Layer Perception	Monthly	Kuala Lumpur, Malaysia	1.932	2.375
(Sanikhani et al., 2018)	Monthly air temperature value between 1901-2010	Extrem Learning Machine	Monthly	Madhya Pradesh, India	2.743	2.269
(Singh et al., 2019)	Weather data collection between 2006-2018	ANN	Monthly	Different airport weather station of India	3.1	-
(Li & Yang, 2023)	Daily ground temperature value between 2012-2021	LSTM	Monthly	Qinhuangdao, China	4.163	3.359
Present Study	Daily air temperature value between 2018-2021	ARIMA(2,1,1)	Monthly (3 rd term)	Afyonkarahisar, Turkey	1.423	1.132

4. Conclusions and Recommendations

Climate change, a global crisis, is causing widespread challenges, ranging from the decline of biodiversity to the depletion of food and water resources. It poses significant threats to human health and leads to ecological imbalances. Increasing urbanization has resulted in higher carbon emissions, improper use of water and agricultural land, and excessive energy consumption, all contributing to the rise in global temperatures. Therefore, it is crucial for all regions, particularly developing countries, to formulate sustainable energy plans and implement effective climate action strategies. In recent years, Turkey has experienced rising temperatures and decreasing precipitation, which could lead to drought and resource scarcity. Regions with continental climates and limited water resources are likely to be the most affected by global warming and climate change. Developing strategies for the effective use of agricultural and water resources is closely linked to temperature variations. Therefore, temperature is a crucial parameter in the climate plans that need to be developed.

Monitoring temperature anomalies plays a key role in protecting water resources, preserving agricultural lands, and implementing sustainable energy projects. In the literature, various studies have been conducted on short-term, medium-term, and long-term temperature forecasting. Methods used include statistical techniques, image-based models, and, more recently, deep neural networks. To achieve higher accuracy, hybrid models are also preferred. However, these hybrid models tend to make the structure of the forecasting model more complex, extend processing times, and increase costs. AI-based deep neural networks are frequently described as "black boxes" due to their lack of transparency and interpretability, which hinders the ability to elucidate the internal mechanisms of the model. In this study, the Box-Jenkins methods was selected for its statistical interpretability, straightforward and flexible model architecture, and its effectiveness in capturing seasonal components. Additionally, The Seasonal Naive Forecast method was chosen as a benchmark approach to evaluate the performance of Box-Jenkins-based ARIMA and SARIMA models and to explicitly reveal the degree of improvement in forecasting accuracy achieved by the developed models.

In this context, the present study focuses on forecasting the daily average temperature for the city of Afyonkarahisar. Due to its location within the TR33 region, Afyonkarahisar serves as a significant hub for the agriculture, industry, and energy sectors. Hourly temperature data, collected from January 1, 2018, to December 31, 2022, were obtained from the meteorological station located in the city center. The ARIMA and SARIMA models have been comparatively evaluated for forecasting air temperature time series. Prior to determining the model parameters, stationarity tests were conducted, and differencing was applied. The ACF and PACF plots of the air temperature time series were utilized to make initial estimations of the parameter values. Various model combinations were tested, leading to the selection of the ARIMA(2,1,1) and SARIMA(2,1,1)x(1,1,2)₁₂ models, which yielded the lowest AIC and BIC values. To analyze the selected models, R-squared plots, histogram distributions, autocorrelation plots, and Q-Q plots were examined. The graphical results indicated that the ARIMA model fits the data more effectively and demonstrates superior generalization capability. Over the past year, performance metrics such as RMSE, MAE, and R-squared were evaluated on a quarterly basis. When the metric results for the four-quarter period were averaged, the SARIMA model yielded an RMSE of 2.2746, an MAE of 1.7434, and an R² value of 0.6867, Sesonal Naive Forecast model yielded an RMSE of 5.157 and MAE of 4.158. In contrast, the ARIMA model showed lower error values with an RMSE of 2.0066 and a MAE of 1.5409, while achieving an improved forecast performance with an R² value of 0.7556. These findings indicate that the ARIMA model captures temperature trends more effectively. The temperature curve in the forecast graphs can provide insights for regions with similar climatic conditions. This information

can help manage water and agricultural resources during periods of increasing temperature. It can also support the development of solar energy projects to promote sustainable energy use.

The aim for future research is to design a multidimensional time series model that includes additional meteorological data as well as historical air temperature values. Optimization of model parameters using optimization algorithms can be targeted to increase forecast accuracy. In addition, conducting a comparative air temperature forecast study for all provinces in the TR33 region will facilitate the development of strategies in the energy and climate fields.

Authors' Contributions

All authors contributed equally to the study.

Statement of Conflicts of Interest

There is no conflict of interest between the authors.

Statement of Research and Publication Ethics

The author declares that this study complies with Research and Publication Ethics.

References

- Akaike, H. (1974). A new look at the statistical model identification. *IEEE transactions on automatic control*, 19(6), 716-723. <https://doi.org/10.1109/TAC.1974.1100705>
- Alencar, D. B. de, Affonso, C. M., Limão de Oliveira, R. C., & Reston Filho, J. C. (2018). Hybrid Approach Combining SARIMA and Neural Networks for Multi-Step Ahead Wind Speed Forecasting in Brazil. *IEEE Access*, 6, 55986–55994. <https://doi.org/10.1109/ACCESS.2018.2872720>
- Alomar, M. K., Khaleel, F., Aljumaily, M. M., Masood, A., Razali, S. F. M., AlSaadi, M. A., ... & Hameed, M. M. (2022). Data-driven models for atmospheric air temperature forecasting at a continental climate region. *PLoS One*, 17(11), e0277079.
- Amjad, M., Khan, A., Fatima, K., Ajaz, O., Ali, S., & Main, K. (2022). Analysis of temperature variability, trends and prediction in the Karachi Region of Pakistan using ARIMA models. *Atmosphere*, 14(1), 88. <https://doi.org/10.3390/atmos14010088>
- Aghelpour, P., Mohammadi, B., & Biazar, S. M. (2019). Long-term monthly average temperature forecasting in some climate types of Iran, using the models SARIMA, SVR, and SVR-FA. *Theoretical and Applied Climatology*, 138(3), 1471-1480.
- Beggs, P. J. (2004). Impacts of climate change on aeroallergens: past and future. *Clinical & Experimental Allergy*, 34(10), 1507–1513. <https://doi.org/10.1111/J.1365-2222.2004.02061.X>
- Box, G. E. P., & Jenkins, G. M. (1970). *Time series analysis: Forecasting and control*. Holden-Day.
- Demirbaş, M., & Aydın, R. (2020). 21. Yüzyılın En Büyük Tehdidi: Küresel İklim Değişikliği. *E-Journal of New World Sciences Academy*, 15(4), 163–179. <https://doi.org/10.12739/NWSA.2020.15.4.5A0143>
- De Saa, E., & Ranathunga, L. (2020). Comparison between arima and deep learning models for temperature forecasting. <https://doi.org/10.48550/arXiv.2011.04452>

- Dickey, D. A., & Fuller, W. A. (1979). Distribution of the estimators for autoregressive time series with a unit root. *Journal of the American statistical association*, 74(366a), 427-431. <https://doi.org/10.1080/01621459.1979.10482531>
- Dinc Cavlak, O. (2024). Sürdürülebilir hisse senedi endekslerinin DCC-GARCH modeli ile incelenmesi ve petrol fiyatlarının bu ilişkiye etkisi. *Afyon Kocatepe Üniversitesi İktisadi Ve İdari Bilimler Fakültesi Dergisi*, 26(1), 48-58. <https://doi.org/10.33707/akuiibfd.1335551>
- Franchini, M., & Mannucci, P. M. (2015). Impact on human health of climate changes. *European Journal of Internal Medicine*, 26(1), 1–5. <https://doi.org/10.1016/J.EJIM.2014.12.008>
- Fu, H.-Z. (2022). A large-scale bibliometric analysis of global climate change research between 2001 and 2018. *Climatic Change*, 170(3–4). <https://doi.org/10.1007/s10584-022-03324-z>
- Haque, E., Tabassum, S., & Hossain, E. (2021). A comparative analysis of deep neural networks for hourly temperature forecasting. *IEEE Access*, 9, <https://doi.org/10.1109/ACCESS.2021.3131533>
- Hamilton, J. D. (2020). *Time series analysis*. Princeton university press.
- Hou, J., Wang, Y., Zhou, J., & Tian, Q. (2022). Prediction of hourly air temperature based on CNN–LSTM. *Geomatics, Natural Hazards and Risk*, 13(1), 1962-1986. <https://doi.org/10.1080/19475705.2022.2102942>
- Huang, Y., Zhao, H., & Huang, X. (2019, February). A prediction scheme for daily maximum and minimum temperature forecasts using recurrent neural network and rough set. In *IOP Conference Series: Earth and Environmental Science* (Vol. 237, No. 2, p. 022005). IOP Publishing. <https://doi.org/10.1088/1755-1315/237/2/022005>
- Islam, M., & Zakaria, M. T. (2019). Forecasting of maximum and minimum temperature in the Cox's Bazar Region of Bangladesh based on time series analysis. *IOSR J. Math. IOSR-JM*, 15, 56-67. <https://doi.org/10.9790/5728-1505035667>
- Joanes, D.N. and Gill, C.A. (1998), Comparing measures of sample skewness and kurtosis. *Journal of the Royal Statistical Society: Series D (The Statistician)*, 47: 183-189. <https://doi.org/10.1111/1467-9884.00122>
- Karabulut, M. A., & Topçu, E. (2022). Derin öğrenme tekniği kullanılarak kars ilinin hava sıcaklık tahmini. *Mühendislik Bilimleri ve Tasarım Dergisi*, 10(4), 1174–1181. <https://doi.org/10.21923/jesd.1067700>
- Kisi, O., & Shiri, J. (2014). Prediction of long-term monthly air temperature using geographical inputs. *International Journal of Climatology*, 34(1), 179–186. <https://doi.org/10.1002/JOC.3676>
- Kwiatkowski, D., Phillips, P. C., Schmidt, P., & Shin, Y. (1992). Testing the null hypothesis of stationarity against the alternative of a unit root: How sure are we that economic time series have a unit root?. *Journal of econometrics*, 54(1-3), 159-178. [https://doi.org/10.1016/0304-4076\(92\)90104-Y](https://doi.org/10.1016/0304-4076(92)90104-Y)
- Lai, Y., & Dzombak, D. A. (2020). Use of the autoregressive integrated moving average (ARIMA) model to forecast near-term regional temperature and precipitation. *Weather and forecasting*, 35(3), 959-976. <https://doi.org/10.1175/WAF-D-19-0158.1>
- Li, G., & Yang, N. (2023). A hybrid sarima-lstm model for air temperature forecasting. *Advanced Theory and Simulations*, 6(2), 2200502.
- Murat, M., Malinowska, I., Gos, M., & Krzyszczak, J. (2018). Forecasting daily meteorological time series using ARIMA and regression models. *International agrophysics*, 32(2). <https://doi.org/10.1515/intag-2017-0007>
- Naing, W. Y. N., & Htike, Z. Z. (2015). Forecasting of monthly temperature variations using random forests. *ARNP journal of Engineering and Applied Sciences*, 10(21), 10109-10112.
- Nketiah, E. A., Chenlong, L., Yingchuan, J., & Aram, S. A. (2023). Recurrent neural network modeling of multivariate time series and its application in temperature forecasting. *Plos one*, 18(5), e0285713. <https://doi.org/10.1371/journal.pone.0285713>
- Ozbek, A., Sekertekin, A., Bilgili, M., & Arslan, N. (2021). Prediction of 10-min, hourly, and daily atmospheric air temperature: comparison of LSTM, ANFIS-FCM, and ARMA. *Arabian Journal of Geosciences*, 14, 1-16. <https://doi.org/10.1007/s12517-021-06982-y>
- Öztürk, K. (2002). Küresel iklim değişikliği ve Türkiye'ye olası etkileri. *Gazi Üniversitesi Gazi Eğitim Fakültesi Dergisi*, 22(1).
- Park, I., Kim, H. S., Lee, J., Kim, J. H., Song, C. H., & Kim, H. K. (2019). Temperature prediction using the missing data refinement model based on a long short-term memory neural network. *Atmosphere*, 10(11), 718. <https://doi.org/10.3390/atmos10110718>
- Polat, E., & Kahraman, S. (2021). Antroposen Çağı'nda pandemi ve kentlerin durumu. 41, 21–31. <https://doi.org/10.33613/ANTROPOLOJIDERGISI.810841>

- Roy, D. S. (2020). Forecasting the air temperature at a weather station using deep neural networks. *Procedia computer science*, 178, 38-46. <https://doi.org/10.1016/j.procs.2020.11.005>
- Salcedo-Sanz, S., Deo, R. C., Carro-Calvo, L., & Saavedra-Moreno, B. (2016). Monthly prediction of air temperature in Australia and New Zealand with machine learning algorithms. *Theoretical and Applied Climatology*, 125(1), 13–25. <https://doi.org/10.1007/S00704-015-1480-4>
- Sanikhani, H., Deo, R. C., Samui, P., Kisi, O., Mert, C., Mirabbasi, R., ... & Yaseen, Z. M. (2018). Survey of different data-intelligent modeling strategies for forecasting air temperature using geographic information as model predictors. *Computers and Electronics in Agriculture*, 152, 242-260.
- Sekertekin, A., Bilgili, M., Arslan, N., Yildirim, A., Celebi, K., & Ozbek, A. (2021). Short-term air temperature prediction by adaptive neuro-fuzzy inference system (ANFIS) and long short-term memory (LSTM) network. *Meteorology and Atmospheric Physics*, 133, 943-959. <https://doi.org/10.1007/s00703-021-00791-4>
- Schwarz, G. (1978). Estimating the dimension of a model. *The annals of statistics*, 461-464.
- Shen, H., Jiang, Y., Li, T., Cheng, Q., Zeng, C., & Zhang, L. (2020). Deep learning-based air temperature mapping by fusing remote sensing, station, simulation and socioeconomic data. *Remote Sensing of Environment*, 240, 111692. <https://doi.org/10.1016/j.rse.2020.111692>
- Singh, S., Kaushik, M., Gupta, A., & Malviya, A. K. (2019, March). Weather forecasting using machine learning techniques. In *Proceedings of 2nd international conference on advanced computing and software engineering (ICACSE)*. <http://dx.doi.org/10.2139/ssrn.3350281>
- Tektaş, M. (2010). Weather Forecasting Using ANFIS and ARIMA MODELS. *Environmental Research, Engineering and Management*, 51(1), 5–10. <https://doi.org/10.5755/J01.EREM.51.1.58>
- Thi Kieu Tran, T., Lee, T., Shin, J. Y., Kim, J. S., & Kamruzzaman, M. (2020). Deep learning-based maximum temperature forecasting assisted with meta-learning for hyperparameter optimization. *Atmosphere*, 11(5), 487. <https://doi.org/10.3390/atmos11050487>
- Tuğaç, Ç. (2022). İKLİM DEĞİŞİKLİĞİ KRİZİ VE ŞEHİRLER. *Çevre Şehir Ve İklim Dergisi*, 1(1), 38-60.
- Turan, E. S. (2018). Türkiye'nin İklim Değişikliğine Bağlı Kuraklık Durumu. *Doğal Afetler ve Çevre Dergisi*, 4(1), 63–69. <https://doi.org/10.21324/DACD.357384>
- Türkeş, M. (1997). Hava ve iklim kavramları üzerine. *TÜBİTAK Bilim ve Teknik Dergisi*, 355, 36-37.
- Türkeş, M. (2000). Hava, İklim, Şiddetli Hava Olayları ve Küresel Isınma. *TC Başbakanlık Devlet Meteoroloji İşleri Genel Müdürlüğü*, 187, 205.
- UNFCCC. (1992). United nations framework convention on climate change.
- Zaytar, M. A., & El Amrani, C. (2016). Sequence to sequence weather forecasting with long short-term memory recurrent neural networks. *International Journal of Computer Applications*, 143(11), 7-11.
- Wang, H., Huang, J., Zhou, H., Zhao, L., & Yuan, Y. (2019). An integrated variational mode decomposition and ARIMA model to forecast air temperature. *Sustainability*, 11(15), 4018. <https://doi.org/10.3390/su11154018>
- Wang, S., & Ma, J. (2023, October). A Novel Ensemble Model for Load Forecasting: Integrating Random Forest, XGBoost, and Seasonal Naive Methods. In *2023 2nd Asian Conference on Frontiers of Power and Energy (ACFPE)* (pp. 114-118). IEEE.
- World Economic Forum. (2022). The global risks report.